

Calculation Of minimum Shaft Bearing Diameter Of ORC Turbine-Generator 100 kW And Analysis Using Finite Element Method

Hana Hermawan*, Arli Guardi, Sakban, Harry Purnama

Research Center for Process and Manufacturing Industry Technology, BRIN, Tangerang Selatan, 15314, Indonesia

*Corresponding author: hana006@brin.go.id

Abstract

This study aims to analyze the strength of a turbine-generator shaft and determine the minimum diameter of the shaft using the Finite Element Method (FEM). The research problem is to ensure the shaft's strength and durability, considering the high rotation speed of the hermetic turbine generator. The methodology involves using FEM and comparing the calculated minimum diameter with the physical properties of stainless steel 420. The research design includes modeling the shaft using SolidWorks and conducting FEM analysis using Ansys Mechanical Structure. The results show that the maximum von Mises stress is 50.6 MPa, which is below the material's yield strength of 345 MPa. The deformation of the shaft is minimal, and the natural frequencies indicate no critical speed below the rated RPM of the turbine-generator. The implications of this study are that the analyzed shaft design is safe and meets the strength requirements for the turbine-generator.

Keywords:

Organic Rankine Cycle, hermetic turbine generator, shaft strength, Finite Element Method (FEM), von Mises stress, deformation, natural frequencies.

1 Introduction

The Organic Rankine Cycle (ORC) involves modifying the conventional Rankine Cycle by replacing steam with an organic fluid to rotate the turbine. A hermetic turbine generator, of which all components are enclosed within a casing, drives a generator on a single shaft to produce electricity.

The turbine generator shaft is an essential component typically installed horizontally, parallel to the working fluid's entry and perpendicular to its exit. Shafts are integral to numerous mechanical systems and transfer power and torque between machine elements [1][2]. They connect rotating parts and provide an axis of rotation, enabling one part to rotate another. Proper shaft design enhance system operation through improved efficiency and safety [3].

The fundamentals of shaft design have been well-documented for decades [4]-[6]. Fadjrln et al. [7] conducted shaft design on the bow thruster electric motor traction, referencing the minimum diameter according to SKF code 29322e. It is important to note that technical abbreviations will be explained upon first use. Liang et al. [8] conducted an objective design for the shaft of an electric motor-powered vehicle by evaluating its strength, critical speed, and stress concentration to determine the motor operation and bearing life expectancy. Rasovic et al. [9] described the shaft design using analytical equations and compared its accuracy

against numerical simulations, revealing less than 10% deviation from equivalent stress and deformation. Munteanu et al. [10] applied the semi-analytical finite element method to design the shaft. They modeled the general loading conditions, including axial, torsional, bending, and shear loads through Fourier series expansion. This approach proved more effective than 3D modeling. Lai et al. [11] conducted a ship propulsion shaft design, optimizing bearing displacement against performance indexes with multi-disciplinary and multi-objective methods. The study demonstrated the potential to enhance the quality and efficiency of the shaft. Further design optimization for the strength of the shaft was attained via numerical simulation to identify the most efficient design regarding assembly time and cost [12].

To minimize the damage caused by vibrations that occur at the critical speed during start-up, it's necessary to perform a natural frequency analysis and determine the turbine's critical speed. The appropriate bearing selection will allow the shaft design of the bearing to determine an appropriate size that is strong enough without being excessive or unsafe during operation[13].

The objective of this study is to present a thorough examination of the design of the shaft, particularly in hermetically sealed turbine generators. The objective of this analysis is to provide a point of reference concerning sturdy shaft systems in hermetic turbines. The design of the shaft has been fortified through analytical equations and numerical analysis. The outcomes, consisting of equivalent stresses, deformations, and possible frequencies, have been acquired.

2 Research Method

At the first stage, determine the distance between bearings on the shaft based on the boundary of generator and turbine dimension. The total length and distance between bearings of the shaft is shown in Fig 1.

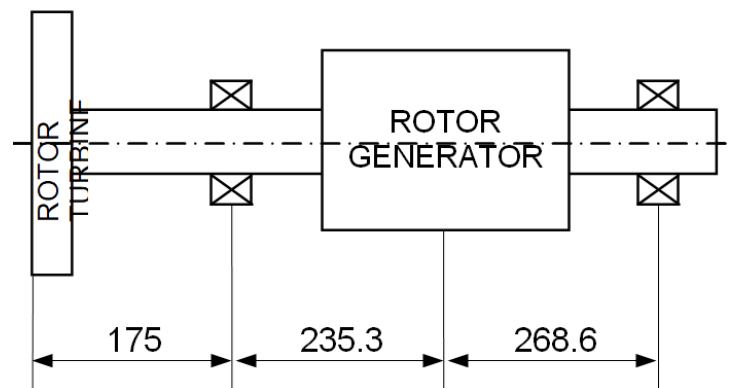


Fig. 1. Distance between bearings.

At the second stage, calculate diameter of the shaft based on data operation parameters of the turbine-generator. The operation parameter is shown in Table 1. The calculation begins by calculating the torque caused by power and rotation, and obtained a torque of 119.4 Nm. Then proceed to calculate the tangential force based on torque and obtain a force of 795.8 N, because the turbine inlet comes from the axial direction of the shaft, the axial force needs to be taken into consideration, by calculating based on the pressure and area of the turbine obtained an axial force of 1237 N. Eq. 1 evaluates torque. In detail T denoted by Torque (NM), P denoted by Power (KW), n denoted by RPM.

Table1. Operation parameters

Item	Value
Power	100 kW
Speed	8000 RPM
Radius turbine	0.15 m
Radius generator	0.0965 m
Inlet turbine pressure	9.8 BarG

Formulas:

1. Torque from power and RPM (Eq. 1)

$$T = \frac{9550 \times P}{n} \quad (1)$$

Where T is torque, P is power and n is RPM.

2. Tangential force (Eq. 2)

$$F = \frac{T}{r} \quad (2)$$

Where F is force (N) and r is radius turbine/generator.

3. Pressure (Eq. 3)

$$P = \frac{F}{A} \quad (3)$$

Where A is area of rotor turbine/generator.

Free body diagram that corresponds to the shear and moment diagram along the shaft as shown in Fig. 2.

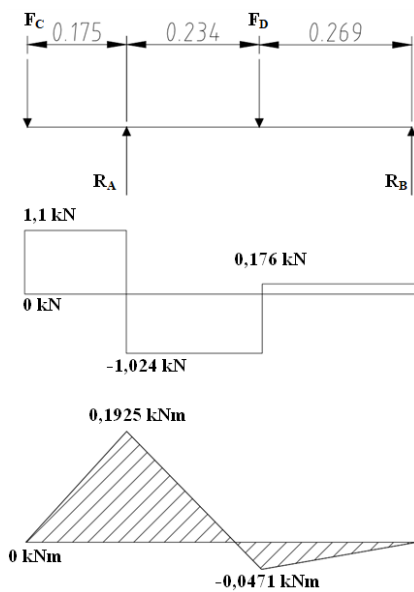


Fig. 2. Shaft free body diagram, shear force and bending moment diagram.

The equations of resultant stress due to axial force and bending moment are shown in Eq. 4 – Eq. 7.

Shaft is subjected to a combination of axial force, bending moment and torsional moment (Eq. 4).

$$\sigma_x = \sigma_t + \sigma_b \quad (4)$$

Permissible value of maximum stress (Eq. 5).

$$\sigma_i = \frac{\sigma_{tu}}{FS} \quad (5)$$

Shaft tensile stress (Eq. 6).

$$\sigma_t = \frac{4P}{\pi d^2} \quad (6)$$

Shaft bending stress (Eq. 7).

$$\sigma_b = \frac{32M_b}{\pi d^3} \quad (7)$$

With these formula, the minimum diameter is 27 mm and to roundup number then 30 mm is selected.

2.1 Safety Factor

Allowable stress is the maximum stress that a system structure withstand without failure, regardless of the location of safety factors. The allowable stress is formulated by Eq. 8.

$$SF = \frac{F_u}{F_{allow}} \quad (8)$$

Where SF denotes safety factor, F_u is ultimate strength and F_{allow} is allowable stress. If SS420 has an ultimate strength of 655 MPa, then the allowable stress is 109.2 MPa.

2.2 Shaft Modeling

The modeling of the shaft is using Solid Works 2021 License as shown in Fig 3.

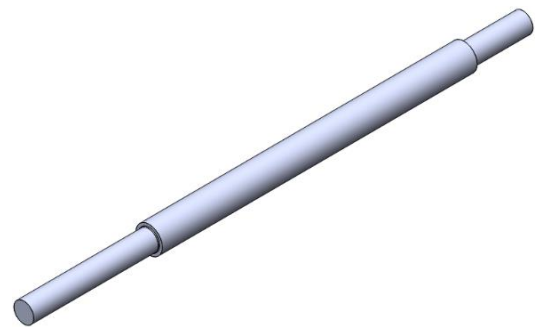


Fig. 3. 3D model shaft.

The next step is solving by finite element method by using Ansys 14.5 Mechanical software. Material properties is set to the properties of the stainless steel 420 as it shown on Fig. 4. Meshing process is a finite element discretization process. To produce a good meshing elements, so global and local meshing must be controlled. The quality of mesh is set to medium span angle center, mesh inflation in smooth inflation, and mesh size is set to 6 mm. Mesh geometry is set to hexagonal dominant. Mesh model is shown in Fig 5.

SS420 mechanical properties in various heat-treated or cold-worked conditions.							
Type (UNS)	Condition	Tensile strength, MPa (ksi), ≤	Yield strength, MPa (ksi), ≤	Elongation in 50.8 mm (2 in.), %, ≥	Reduction in area, %, ≥	Hardness	Charpy V-notch impact strength, J (ft-lbf)
AISI 420 (UNS S42000)	Oil quenched from 1038 °C (1900 °F) and tempered at 316 °C (600 °F)	1724 (250)	1482 (215)	8	25	52 HRC, Rockwell, ≥	20 (15), ≥
	Annealed bar	655 (95)	345 (50)	25	55	195 HBW, Brinell, ≤	–
	Annealed and cold drawn	760 (110)	690 (100)	14	40	228 HBW, Brinell, ≤	–

Fig. 4. Material properties are set to the properties of the stainless steel 420.

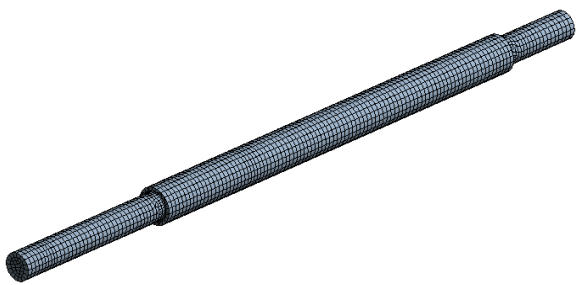


Fig. 5. Meshing shaft.

The third step is to set the boundary condition. This condition including loading and support area. The shaft was supported by two bearing in front and rear area of rotor generator. In this case, support is using fixed support in bearing area to set that the shaft is held to be stationary, then twisted by the moment load with opposite direction between moment from rotor turbine in clockwise and moment from rotor generator in counterclockwise direction in orientation look from front of the turbine.

The loading conditions in this case is ignore mechanical vibration and the shaft is not affected by the frictional force of the ball bearing. Boundary condition is shown in Fig. 6 and loading details is shown in Table 2.

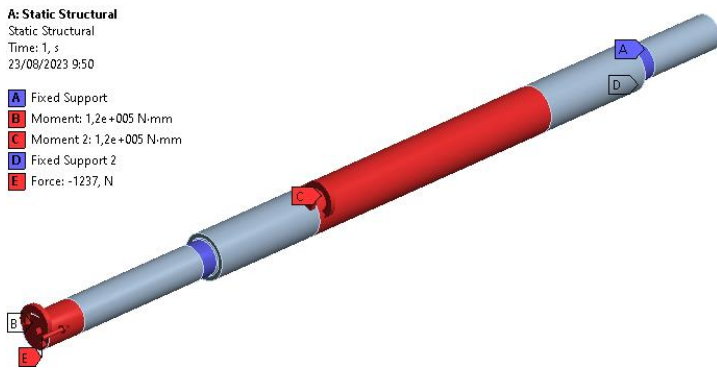


Fig. 6. Boundary condition.

Table 2. Value of boundary condition

Loadings	Value
Cylindrical support	Fixture
Cylindrical support	Fixture
Load turbine	120 Nm
Load generator	-120 Nm
Axial force	1237 N

3 Results and Discussion

3.1 Pre-Processing Mesh

The discretization of the shaft model structure is represented in a mesh consisting of nodes and elements. The mesh results are fully defined based on meshing process with nodes value is 48398 elements and the number of mesh elements are 12493 elements. The numbers of element and node are shown in Fig. 7.

Statistics	
<input type="checkbox"/> Nodes	48398
<input type="checkbox"/> Elements	12493

Fig. 7. Meshing statistics.

3.2 Von-Mises Stress

Von Mises stress is a value used to determine if a given material will yield or fracture[14]. It is mostly used for ductile materials, such as metals. The von Mises yield criterion states that if the von Mises stress of a material under load is equal to or greater than the yield limit of the same material under simple tension then the material will yield and has been used as one of the most reliable failure criteria for engineering materials.

Von-Mises stress distribution of the shaft is shown in Fig. 8. The maximum stress that occurs at the shaft by applying the load is 50.6 which located in near bearing area, and the minimum stress is 3×10^{-9} MPa. The maximum stress is far below the material yield strength as shown in Fig. 4 that stainless steel 420 has is 345 MPa.

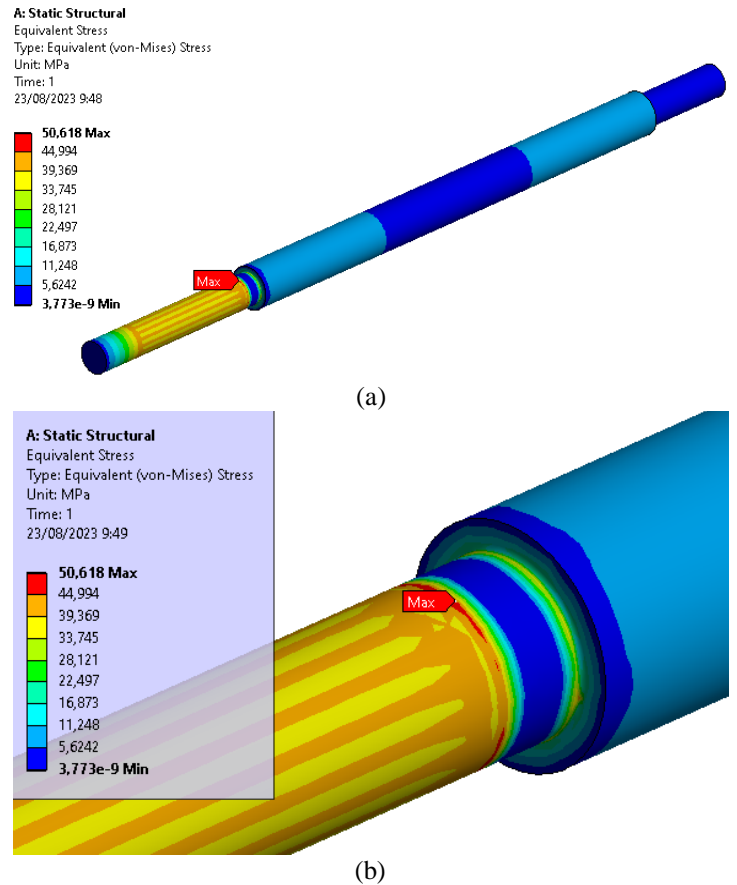


Fig. 8. Von-misses stress of the shaft.

3.3 Deformation

Deformation mainly happens due to stress which be said a force applied to the specific area. The deformation value and distribution of the shaft is shown in Fig. 9 with the maximum value is 0.047 mm which is located in turbine area and the direction is in y axis. Compare to the deformation criteria of the material of the shaft is still far below from the maximum value.

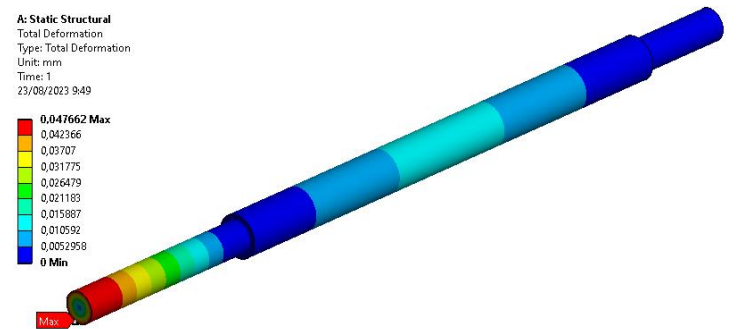


Fig. 9. Deformation of the shaft.

3.4 Modal Analysis

Modal analysis is providing the natural frequencies at which a structure will resonate[15]. These natural frequencies are of paramount importance in various engineering fields, For instance, when designing a machine's structure or components.

In order to determine the frequencies at which components will resonate, it is important to have knowledge of their natural frequencies. Additionally, understanding the critical speed of the turbine be helpful in quickly bypassing it during startup until it reaches its rated RPM. Modal analysis requires inserting a 3D model, meshing, applying boundary conditions, solving, developing modes, and evaluating results.

The Table 3 lists the first six natural frequencies of the model, and Fig. 10 shows the corresponding graphic. There is no critical speed below the rated 8000 RPM of the turbine-generator as the frequencies convert to RPM.

Table 3. Natural frequencies to RPM

Mode	Freq. (Hz)	RPM
1	682.46	40947.6
2	682.73	40963.8
3	689.23	41353.8
4	689.56	41373.6
5	1851.1	111066

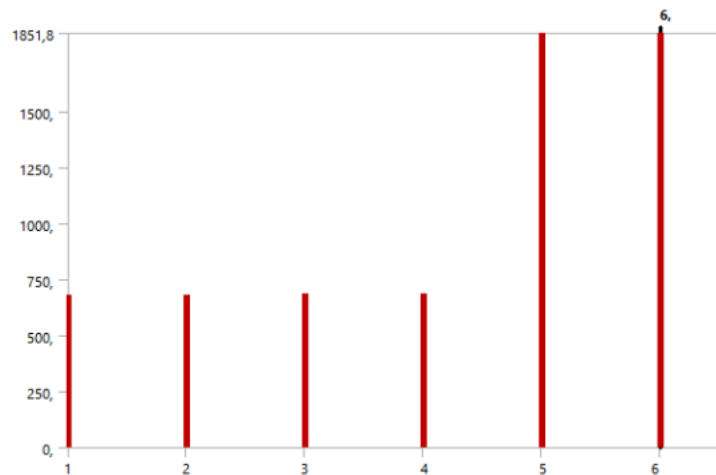


Fig. 10. The first sixth natural frequencies of the shaft.

4 Conclusion

This study has discussed the calculation of the minimum bearing diameter of a shaft in turbine-generator and analyzed the strength of the shaft due to operational load using the Finite Element Method (FEM). The FEM results were visually represented by von-Mises stress and deformation. The maximum stress was found to be near the front bearing, and its value is 50.6 MPa which is half of the allowable stress, and causing only a small deformation that is far less than 1 mm. The natural frequency results indicated that there are no frequencies under the rated RPM of the turbine, which means that there is no critical speed when the turbine starts up. Therefore, the bearing diameter is safe to use.

References

- [1] R. L. Mott, *Machine elements in mechanical design*. Pearson Educación, 2004.
- [2] P. R. N. Childs, *Mechanical Design: Theory and Applications*. Butterworth-Heinemann, 2021.
- [3] D. Zhao, H. Tu, Q. He, and H. Li, "Research on the Design and Construction of Inclined Shafts for Long Mountain Tunnels: A Review," *Sustainability*, vol. 15, no. 13, p. 9963, 2023.
- [4] G. D. Redford and G. D. Redford, "Application of Simple Stresses," *Mech. Eng. Des. An Introd.*, pp. 125–160, 1966.
- [5] G. & F. Holl EG**, "A review of some aspects of shaft design," *J. South. African Inst. Min. Metall.*, vol. 73, no. 10, pp. 309–324, 1973.
- [6] K. F. Unrug, "Shaft design criteria," *Int. J. Min. Eng.*, vol. 2, pp. 141–155, 1984.
- [7] B. N. Fadjarin, H. Purnama, M. I. Adhynugraha, and C. S. A. Nandar, "Shaft Mechanical Design of 250 kW Electric Motor," in *Proceedings of 2018 International Conference on Electrical Engineering and Computer Science, ICECOS 2018*, 2019. doi: 10.1109/ICECOS.2018.8605227.

- [8] J. Liang, J. W. Jiang, B. Bilgin, and A. Emadi, "Shaft design for electric traction motors," *IEEE Trans. Transp. Electr.*, vol. 4, no. 3, pp. 720–731, 2018.
- [9] N. Rašović, A. Vučina, and R. Dedić, "Design and analysis of steel reel shaft by using FEA," *Teh. Vjesn.*, vol. 26, no. 2, pp. 527–532, 2019.
- [10] M. G. Munteanu, F. De Bona, and F. Bressan*, "Shaft design: A semi-analytical finite element approach," *Mech. Based Des. Struct. Mach.*, vol. 46, no. 2, pp. 184–195, 2018.
- [11] G. Lai *et al.*, "Numerical and experimental study on comprehensive optimization for the KPIs of ship propulsion shafting design based on MDO," *Ocean Eng.*, vol. 222, p. 108624, 2021.
- [12] H. Song, J. Zhang, and F. Zhang, "Rotor strength and critical speed analysis of a vertical long shaft fire pump connected with different shaft lengths," *Sci. Rep.*, vol. 12, no. 1, p. 9351, 2022.
- [13] E. DwiPurnomoet *al.*, "Analysis of BLDC Electric Motor Shaft Treatment Model Using Numerical Method," *MajalahIlmiahPengkajianIndustri (Journal of Industrial Research and Innovation)*, vol. 16, no. 1, pp. 30–35, 2022.
- [14] Ravikant, G. Krishan, and M. Didwania, "Modal analysis of drive shaft using FEA," *International Journal of Engineering and Management Research*, vol. 3, pp. 4–7, Feb. 2013.
- [15] K. Sathishkumar and N. Ugesh, "FINITE ELEMENT ANALYSIS OF A SHAFT SUBJECTED TO A LOAD," 2016. Online]. Available: www.arpnjournals.com